

3 **Advancing Plant Biomass Measurements: Integrating**
4 **Smartphone-based 3D Scanning Techniques for Enhanced**
5 **Ecosystem Monitoring**

6 Peter Dietrich^{1,2 α *}, Melanie Elias^{3 α *}, Peter Dietrich^{4,5,2}, Stanley Harpole^{2,6,7},
7 Christiane Roscher^{2,6}, Jan Bumberger^{8,4,2}

8 ^{α} shared first authorship

10 ¹Geobotany and Botanical Garden, Martin Luther University Halle-Wittenberg, Halle (Saale),
11 Germany

12 ²German Centre of Integrative Biodiversity Research (iDiv) Halle-Jena-Leipzig, Leipzig,
13 Germany

14 ³Institute of Photogrammetry and Remote Sensing (IPF-TUD), Dresden University of
15 Technology, Dresden, Germany

16 ⁴Department of Monitoring and Exploration Technologies, Helmholtz Centre for
17 Environmental Research (UFZ), Leipzig, Germany

18 ⁵University of Tübingen, Geo- and Environmental Sciences, Tübingen, Germany

19 ⁶Department Physiological Diversity, Helmholtz Centre for Environmental Research (UFZ),
20 Leipzig, Germany

21 ⁷Martin Luther University Halle-Wittenberg, Halle (Saale), Germany.

22 ⁸Research Data Management - RDM, Helmholtz Center for Environmental Research (UFZ),
23 Leipzig, Germany

24 *Corresponding Authors: peter.dietrich@botanik.uni-halle.de, melanie.elias@tu-dresden.de

26 ORCID

27 Peter Dietrich (MLU) 0000-0002-7742-6064

28 Melanie Elias (IPF-TUD) 0000-0003-2169-8762

29 Peter Dietrich (UFZ) 0000-0003-2699-2354

30 Stanley Harpole 0000-0002-3404-9174

31 Christiane Roscher 0000-0001-9301-7909

32 Jan Bumberger 0000-0003-3780-8663

34 **Abstract**

35 New technological developments open novel possibilities for widely applicable methods of
36 ecosystem analyses. We investigated a novel approach using smartphone-based 3D scanning
37 for non-destructive, high-resolution monitoring of above-ground plant biomass. This method
38 leverages Structure from Motion (SfM) techniques with widely accessible smartphone apps and
39 subsequent computing to generate detailed ecological data. By implementing a streamlined
40 pipeline for point cloud processing and voxel-based analysis, we enable frequent, cost-effective,
41 and accessible monitoring of vegetation structure and plant community biomass. Conducted in
42 long-term experimental grasslands, our study reveals a high correlation (R^2 up to 0.9) between
43 traditional biomass harvesting and 3D volume estimates derived from smartphone-generated
44 point clouds, validating the method's accuracy and reliability. Additionally, results indicate
45 significant effects of plant species richness and fertilization on biomass production and volume
46 estimates, underscoring the potential for high-resolution temporal and spatial analyses of
47 vegetation dynamics. This method's innovation extends beyond traditional practices with
48 implications for future integration of AI to automate species segmentation, ecological trait
49 extraction, and predictive modeling. The simplicity and accessibility of the smartphone-based
50 approach facilitate broader engagement in ecosystem monitoring, encouraging citizen science
51 participation and enhancing data collection efforts. Future research will make it possible to
52 refine the accuracy of point cloud processing, expand applications across diverse vegetation
53 types, and explore new possibilities in ecological monitoring, modeling, and its application in
54 ecosystem analyses and biodiversity research.

55

56 **Keywords:** biodiversity, photogrammetry, Scaniverse, vegetation height, vegetation structure

57 **Introduction**

58 Biodiversity is declining dramatically due to the effects of global change, with unknown
59 consequences for human life on Earth (Cardinale *et al.* 2012; Keesing & Ostfeld 2021;
60 Habibullah *et al.* 2022). In recent years, more and more research has been carried out on this
61 topic in order to better predict the consequences of global change and to understand its
62 underlying processes. Flagships of such research are biodiversity experiments, such as Cedar
63 Creek (Tilman *et al.* 1997) and the Jena Experiment (Weisser *et al.* 2017), globally distributed
64 experimental studies in natural grasslands, such as Drought Network (Smith *et al.* 2024), or the
65 Nutrient Network (Borer *et al.* 2014), and research infrastructures along natural diversity or
66 land-use gradients like the Biodiversity Exploratories (Fischer *et al.* 2010) or TERENO in
67 Germany (Zacharias *et al.* 2024) and eLTER in Europe (Mollenhauer *et al.* 2018; Ohnemus *et*
68 *al.* 2024).

69 A common variable studied in these research facilities is above-ground plant biomass, serving
70 as a proxy for plant productivity, which is a fundamental component of ecosystem functioning.
71 The most frequent method to determine above-ground biomass is to harvest the plants at ground
72 level on a defined area, followed by drying and weighing (there are also alternative non-
73 destructive methods (López-Díaz, Roca-Fernández & González-Rodríguez 2011), which are,
74 however, used comparatively rarely).

75 Despite its simplicity and relatively low cost, the harvest method has notable limitations:
76 repeated destructive biomass harvest can change plant growth and can therefore not be repeated
77 in short time intervals on permanent plots. Estimating actual productivity, which entails
78 measuring rates of biomass change rather than just the standing stock, however, requires long-
79 term series of biomass data over multiple seasons. Furthermore, destructive sampling offers
80 only a coarse temporal and spatial resolution, limiting the ability to capture detailed variation
81 in vegetation structure.

82 In recent years, advanced and modern techniques have emerged, allowing for higher resolution
83 temporal and spatial measurements through 3D scanning and computational analysis of
84 resulting digital point clouds (Lausch *et al.* 2020; Kolhar & Jagtap 2023). Active sensing
85 methods are often summarized as “LiDAR” (Light Detection And Ranging) and include among
86 others airborne (ALS), mobile (MLS) and terrestrial laser scanning (TLS), which have become
87 well established for high-precision 3D vegetation mapping, especially in forestry applications
88 (Bienert *et al.* 2021; Demol *et al.* 2022; Richter & Maas 2022; Bienert *et al.* 2024). However,
89 laser scanning has one decisive disadvantage: the required equipment and software are
90 prohibitively expensive and often inaccessible to many researchers. Passive / optical sensing
91 methods using cameras are of particular interest in today’s on-site crop growth monitoring.
92 Alternative optical methods include the light-field measurement approach (Schima *et al.* 2016;
93 Hu *et al.* 2023), which, while innovative, currently lacks commercially available cameras
94 suitable for this purpose. Another approach is stereoscopy, which derives structural vegetation
95 properties, although it requires calibrated permanent installations and continuous power supply
96 (Dandrifosse *et al.* 2020; Kobe *et al.* 2024).

97 An additional promising method is Structure from Motion (SfM), which uses standard cameras
98 to derive the structural properties of plant communities (Cooper *et al.* 2017; Kröhnert *et al.*
99 2018; Enterkine *et al.* 2023). This technique holds significant potential for extracting structural
100 features of plant communities at the plot level (Enterkine *et al.* 2023). There are already some
101 approaches using this technique for ecosystem monitoring, but they usually involve expensive
102 photo cameras and rather complex processing methods (Enterkine *et al.* 2023). Here we present
103 a new approach that makes the SfM method easily accessible to everyone (i.e., inexpensive and
104 simple to implement) by using a smartphone and freely available 3D scanning apps. Given that
105 nearly everyone owns a smartphone, and that smartphone camera technology has seen rapid
106 advancements in recent years, we see huge potential for ecosystem monitoring. Modern
107 smartphones come with features such as multiple lenses, image stabilisation, autofocus, and

108 cameras with at least 40 megapixels, capable of producing high-resolution images comparable
109 to those taken with SLR cameras. The high quality of today's smartphone camera images
110 enables photogrammetric image processing, e.g. using SfM (Micheletti, Chandler & Lane 2015;
111 Vinci *et al.* 2017; Luetzenburg, Kroon & Bjørk 2021). In a recent study by Chiappini *et al.*
112 (2024), the authors compared the accuracy of 3D urban olive tree models generated including
113 SfM models generated from smartphone images against models from professional MLS. While
114 smartphone-based methods underestimated larger trees, they demonstrated potential as cost-
115 effective alternatives for urban tree assessments, despite limitations in accuracy compared to
116 high-end devices.

117 Beyond the hardware, the software side has also evolved significantly. Freely available apps
118 such as Scaniverse (Niantic Inc., San Francisco, CA, US) or Polycam (Polycam, San Francisco,
119 CA, US) now enable users to perform 3D scans of above-ground vegetation. The process is
120 straightforward: users simply open the app, scan the vegetation, and the app processes the
121 captured images (which takes about 1-2 minutes) before generating a point cloud. This point
122 cloud can then be used to estimate vegetation variables, such as growth height and biomass
123 production. This approach allows for repeated, low-cost, and non-invasive data collection at
124 daily, weekly, or monthly intervals, providing a more accurate and detailed monitoring of plant
125 communities. This can be, for example,

- 126 • temporal dynamics - regular or even automated sampling enables estimates of biomass
127 production rates and growth strategies over time,
- 128 • vegetation structure and spatial variation - 3D point clouds enable a detailed analysis of
129 vegetation structure, including spatial heterogeneity,
- 130 • phenological patterns - by capturing changes in colour, greening and flowering
131 phenology can be quantified.

132 Moreover, the ability to scan plants with smartphones opens up numerous possibilities for
133 citizen science, i.e., people can collect data and provide important additional quantitative and

134 qualitative information (Koedel *et al.* 2022; von Gönner *et al.* 2023). Other conceivable uses
135 would be the investigation of protected or sensitive plant communities through time (Tirrell *et*
136 *al.* 2023) where harvesting is not permitted or possible, or for teaching, in order to better explain
137 structural interrelationships.

138 In the present work we tested whether 3D scans with smartphones generally produce similar
139 results to those of traditional biomass harvesting in a long-term grassland experiment. As part
140 of this research, we aim to provide initial guidance on optimal ways to scan vegetation with a
141 smartphone and, in particular, how to subsequently process the resulting point clouds to
142 generate biomass-like data.

143

144 **Materials and methods**

145 **Study site**

146 The study was conducted in experimental grasslands (DivResource experiment) established at
147 the Feld Station of the Helmholtz Centre for Environmental Research (UFZ) in Bad Lauchstädt,
148 Germany (51°23'38" N, 11°52'45" E, 118 m a.s.l.) in 2011 (Siebenkäs, Schumacher & Roscher
149 2016). The site has an average annual temperature of 9.5°C and 492 mm of precipitation (1981-
150 2010). Eight perennial plant species (four herbs, four grasses), typical of Central European
151 mown grasslands, were selected and divided into two independent species pools. Sown species
152 richness levels are 1, 2 and 4 with paired fertilized and unfertilized experimental plots,
153 respectively. Plots of 2 × 2 m area (later reduced to 1 × 1 m) and arranged in four experimental
154 blocks were weeded three times per year to maintain the sown species combinations. The
155 experiment was mown twice annually (early June, September) and the mown biomass was
156 removed. Fertilization (NPK as pellets, 120:52:100 kg ha⁻¹ yr⁻¹) was applied distributed with
157 two even doses (March, and June after first mowing) from 2012 to 2023.

158

159

160 **3D scans and biomass sampling**

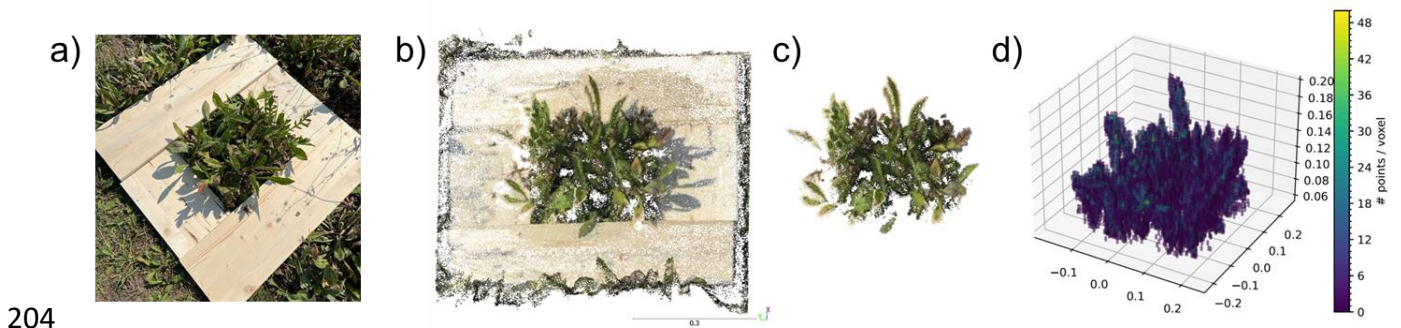
161 On 4 September 2024, we scanned the vegetation in the monocultures and 4-species plots of
162 one species pool, i.e, two monoculture plots of *Lolium perenne* L., *Dactylis glomerata* L.,
163 *Prunella vulgaris* L. and *Knautia arvensis* (L.) Coulter, respectively, and four plots containing
164 all four species (Siebenkäs, Schumacher & Roscher 2016). To do this, we used a frame with a
165 0.3×0.3 m inner surface (made of 0.25 m wide planks; Fig. 1a) to define a specific sub-area
166 per plot (position was randomly chosen in the plot with a sufficient distance from the plot edge).
167 We then used an iPhone 15 Pro and the app Scaniverse to scan the defined area. The Scaniverse
168 app, which is available for free download from the Apple Store and Google Play Store, was
169 preferred to alternatives such as Polycam due to its easy handling, fast scanning speed and high-
170 quality results.

171 For scanning, Scaniverse offers two scan modes: ‘Splat’ and ‘Mesh’. It is very likely that the
172 splat option uses a Gaussian splatting approach to generate 3D representations. With Gaussian
173 splatting, only a small number of 3D points need to be generated from images, with each point
174 having a coordinate in 3D space as well as colour and depth information. Using the Gaussian
175 splats, imaginable as a kind of modifiable bubbles, the appearance of the scanned space can be
176 reconstructed from these points by changing the splats depending on the point attributes. By
177 default, no new real 3D information is generated that can be used for measurement purposes.
178 Mesh-based 3D models are explicitly defined by geometric information, i.e., points, edges, and
179 surfaces. A high-quality mesh that also performs well in visualization is therefore associated
180 with a high-quality and dense 3D point cloud. Consequently, it stands to reason that the mesh
181 function would generate a higher point density.

182 For scanning, we thus first selected the ‘Mesh’ mode and ‘Small Object’ (recommended for
183 objects at a size of “pets, toys and flowers” and likely to predefine the measurement volume),
184 and then scanned the area by capturing the vegetation from all possible angles and distances
185 until the app no longer indicated any red-marked areas in the scan. The scanning took one to

186 two minutes, depending on the density of the vegetation. Each plot was scanned three times.
187 After scanning, we used the ‘Detail’ processing mode to generate the point cloud. This mode is
188 recommended to get the most detailed 3D information. During the ‘Detail’ processing stage,
189 various status messages are displayed, i.e., ‘Aligning Images, Computing Depth, Texturing’,
190 which point to the workflow of SfM. First, the image orientation parameters are determined
191 within the sequence. This is followed by dense matching to compute depth information, i.e., 3D
192 points, through depth triangulation. The calculated 3D points are subsequently textured by the
193 image data. It is important to note that SfM does not inherently provide scale information.
194 Scaniverse probably uses some kind of visual odometry to determine the image trajectory in a
195 metrically scaled coordinate system. This information can be used in the SfM process during
196 image orientation to obtain true-to-scale 3D points in subsequent dense matching. The model
197 was then saved and exported in .ply format (Fig. 1b), that is widely used in the 3D community,
198 using the ‘Share’ function.

199 After scanning, the maximum height of the vegetation in the 0.3×0.3 m sub-plot was measured
200 (vegetation height), and finally plants were harvested 3 cm above the ground (i.e., at height of
201 the wooden frame; which is common for harvesting biomass in such grassland experiments).
202 Biomass was weighed before (fresh biomass) and after (dry biomass) drying for 48h at 60°C .
203

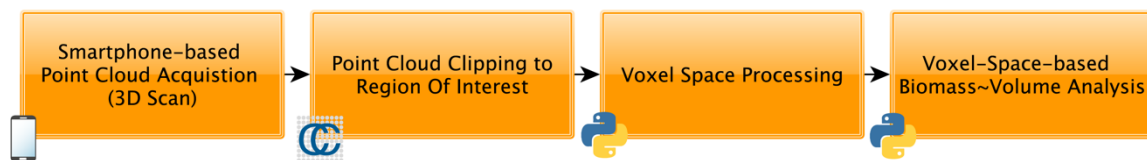


204
205 **Fig. 1** Vegetation in the field with the wooden frame around (a), original point cloud from
206 Scaniverse (b), clipped point cloud (c) used for voxel space calculation (d). Illustrated is a
207 fertilized 4-species mixture plot (voxel size 5 mm).

208 Point cloud and voxel space processing

209 First, the 3D point clouds were processed using CloudCompare, a free software for visualizing
210 and editing point clouds (CloudCompare (version 2.13.2) [GPL software], 2024, retrieved from
211 <http://www.cloudcompare.org/>). Each point cloud was manually clipped to focus on the region
212 of interest, specifically removing all 3D points associated with the structure of the wooden
213 frame and all extraneous 3D points (Fig. 2). In addition, 3D points with height values below the
214 height of the top board layer were excluded to focus only on 3D points on plant parts at least
215 3 cm above soil surface consistent with the cutting height of biomass (Fig. 1c). Future versions
216 of this process could be automated, possibly using e.g. the Python wrapper CloudComPy.

217



218

219 **Fig. 2** Workflow description: after point cloud acquisition via smartphone, point clouds were
220 clipped, voxel space was processed, and finally, relationships between resulting voxel volumes
221 and the harvested biomass were evaluated.

222

223 Voxel data analyses

224 To quantify spatial distributions and characteristics within 3D point clouds, we implemented a
225 voxel-based analysis using Open3D (version 0.18.0) in Python (version 3.10, Fig. 2). Each point
226 cloud was processed into a voxel grid representation at a resolution of 2.5, 5.0, 7.5 and 10.0 mm³
227 per voxel (Fig. 1d). The voxel size is directly related to derived geometric quantities such as
228 volume and height, which is why different voxel sizes were tested, and the derived statistical
229 parameters were compared with conventional measurements to find the most suitable size
230 (Enterkine *et al.* 2023). The voxel grid was generated, respectively, by dividing the spatial

231 domain into cubic voxels of the defined size. The number of points contained within each voxel
232 was then calculated and stored, facilitating density analysis across the scanned region.
233 Voxel-based statistics were computed, including mean, median, and standard deviation of the
234 point count per voxel to describe spatial distribution patterns. Estimates of total volume were
235 derived based on the number of occupied voxels (of known volume - volume is the biomass-
236 like variable), while the maximum vertical height of occupied voxels along the z-axis within
237 each voxel dataset was measured to indicate the height of the structure. For visualization, voxel
238 data that met certain density thresholds were rendered using Python's Matplotlib, with a color
239 map representing voxel point densities. The approach enabled an efficient analysis of point
240 cloud density and volumetric characteristics, providing insights into spatial heterogeneity
241 within the scanned region. In terms of reliability, we averaged the heights and volumes
242 determined per plot (from the three repeated scans) and voxel size for the statistical analyses.
243 The original image data, the clipped image data, as well as the data processing scripts within a
244 Jupyter Notebook, are published under an CC BY 4.0 license at Elias, Dietrich and Bumberger
245 (2024) and can be reused accordingly.

246

247 **Statistical analyses**

248 First, we tested whether species richness and fertilisation history have the same effects on
249 sampled biomass (fresh/dry) and on the determined volumes obtained from the 3D scans (with
250 different voxel size). For this, we used linear mixed-effects models with biomass or volume
251 (derived from voxel sizes 2.5, 5, 7.5 and 10 mm³) as response variable (in single models),
252 species richness, fertilisation history and their interaction as fixed effects and block as random
253 effect. We started with a null model with the random effect only, and then extended the model
254 stepwise by adding the fixed effects (first species richness, then fertilization history and finally
255 the interaction of species richness and fertilization history). Mixed-effects models were fitted

256 with maximum likelihood (ML), and likelihood ratio tests were used to compare models and
257 assess the significance of the fixed effects.

258 In a second step, we tested whether biomass (fresh/dry) and determined volumes (derived from
259 voxel sizes 2.5, 5, 7.5 and 10 mm³) as well as the measured height and the determined height
260 obtained from the 3D scans show significant relationships. For this we used the same mixed
261 effects-model structure as above. For biomass~volume analysis we used fresh or dry biomass
262 as response variable and volume (voxel sizes 2.5, 5, 7.5 and 10 mm³, respectively) as fixed
263 effect, and for height we used measured height as response variable and determined height from
264 3D scans as fixed effect. By visually analysing the regression between measured and
265 determined height, we recognised a potential outlier (one grass monoculture). For this reason,
266 we conducted the height analysis once with and once without this plot.

267 All analyses were performed with the statistical software R (version 3.6.1, R Development Core
268 Team, <http://www.R-project.org>). For linear mixed-effects models, we used the lmer function
269 in the R package lme4 (Bates *et al.* 2014). To calculate R² of regressions, we used the
270 r.squaredGLMM function of R package MuMIn (Barton & Barton 2015).

271

272 **Results**

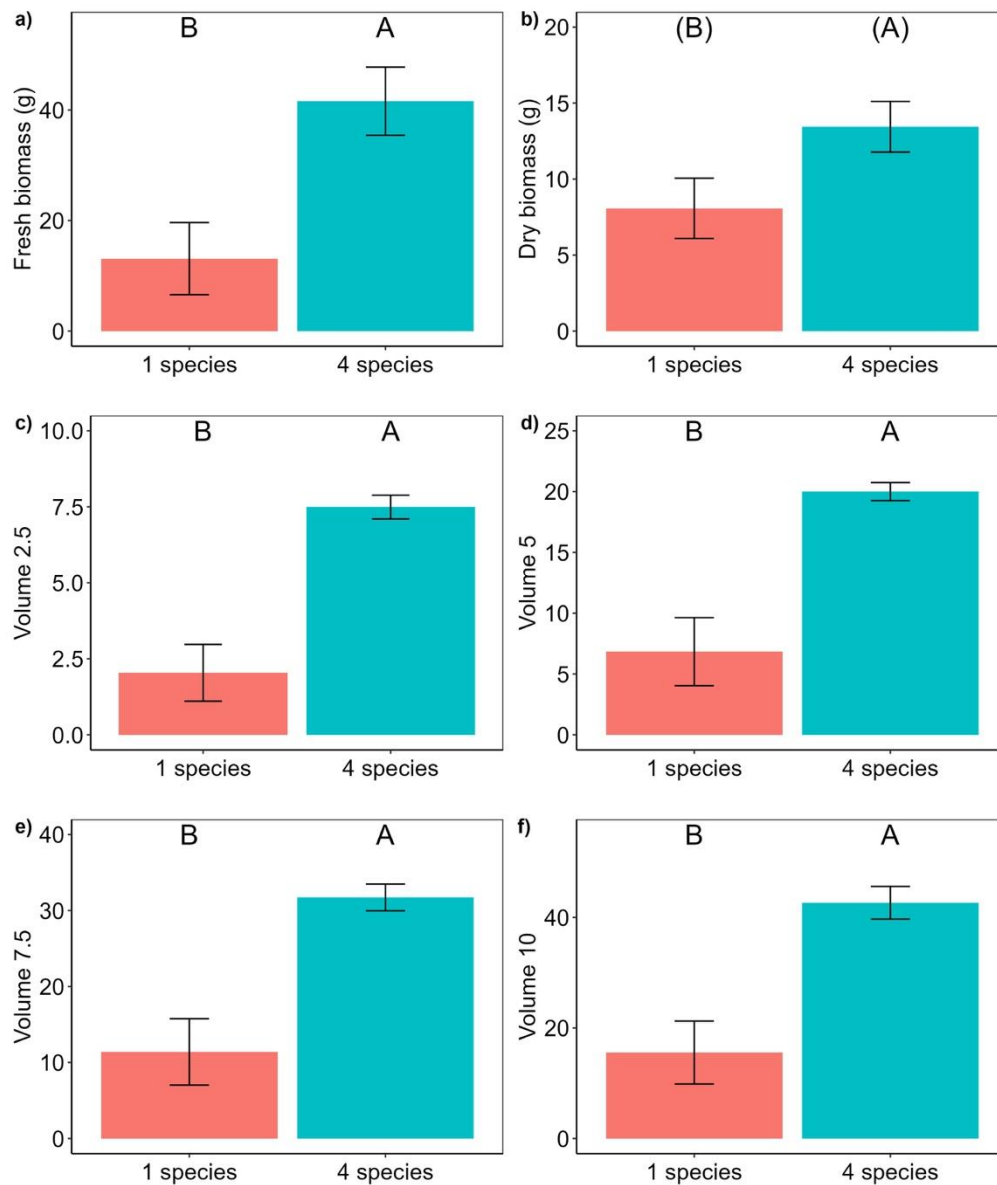
273 **Effects of plant species richness and fertilization history**

274 We found an overall positive effect of plant species richness on aboveground biomass, i.e., four-
275 species mixtures produced more biomass than monocultures (Table 1; Fig. 3a, b). Fertilization
276 history also showed a tendency to increase biomass (Fig 4a, b), while this effect was only
277 marginally significant for dry biomass (Table 1). The interaction between species richness and
278 fertilization history did not have any influence (Table 1). We found similar effects of species
279 richness and fertilization history on the determined volumes obtained from the 3D scans (Table
280 1; Fig. 3c-f, 4c-f).

281 **Table 1** Results of mixed-effects model analyses testing the effects of plant species richness
 282 (SR), fertilization history (Fert.), and their interaction on biomass (fresh and dry) and volume
 283 measurements (voxel size: 2.5, 5, 7.5 and 10 mm³). Shown are degrees of freedom (DF), Chi²
 284 values (χ^2) and P values.

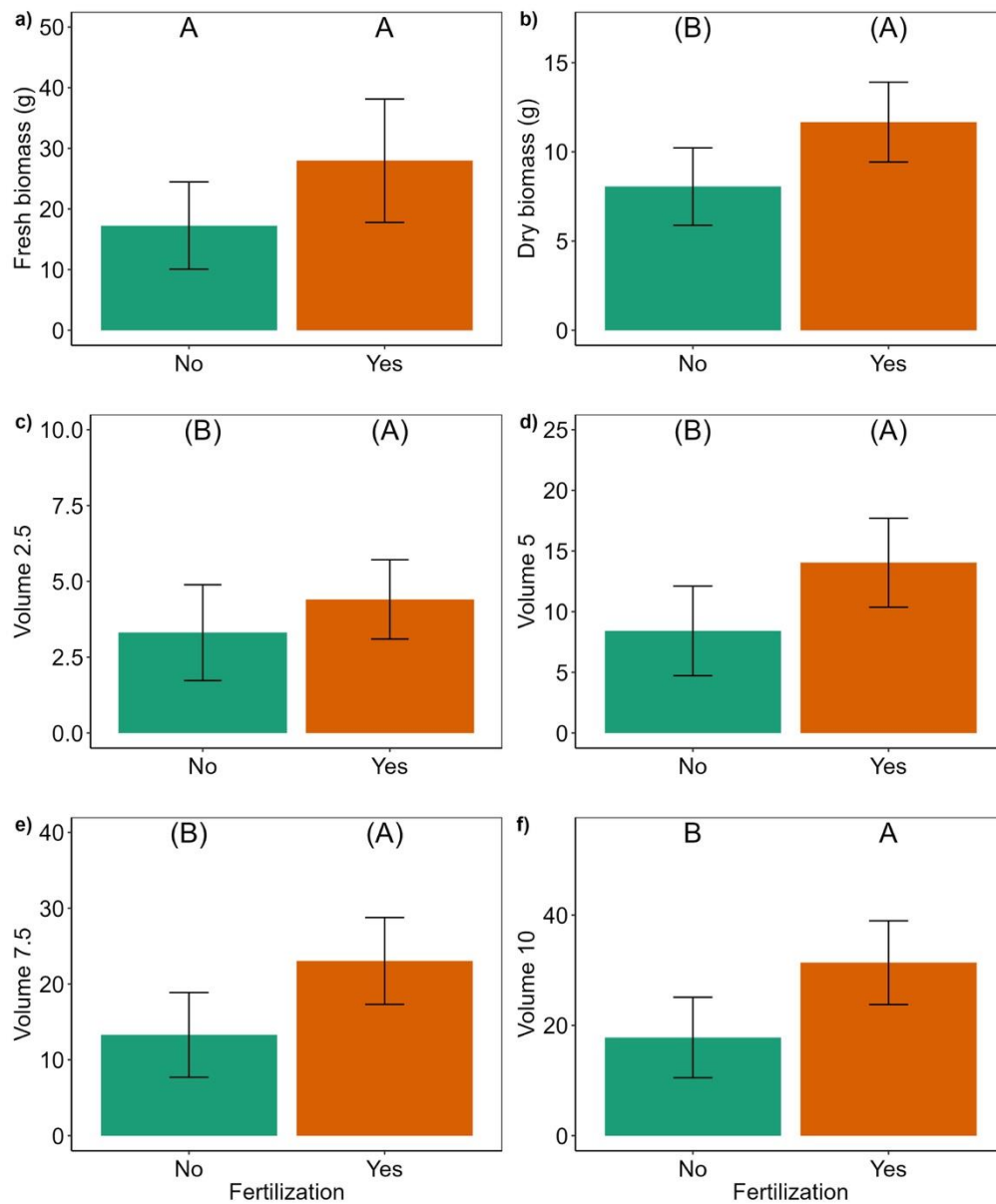
	DF	Fresh biomass		Dry biomass	
		χ^2	P	χ^2	P
Plant species richness (SR)	1	6.80	0.009	3.78	<i>0.052</i>
Fertilization history (Fert.)	1	2.25	0.133	2.70	<i>0.100</i>
SR x Fert.	1	0.68	0.410	0.24	0.627
	DF	Volume 2.5		Volume 5	
		χ^2	P	χ^2	P
Plant species richness (SR)	1	6.50	0.011	5.62	0.018
Fertilization history (Fert.)	1	2.78	<i>0.096</i>	3.22	<i>0.073</i>
SR x Fert.	1	0.13	0.715	0.22	0.640
	DF	Volume 7.5		Volume 10	
		χ^2	P	χ^2	P
Plant species richness (SR)	1	5.50	0.019	5.57	0.018
Fertilization history (Fert.)	1	3.67	<i>0.055</i>	4.05	0.044
SR x Fert.	1	0.22	0.642	0.23	0.628

285



286

287 **Fig. 3** Fresh and dry biomass (a, b), and volume values obtained from voxel analysis with voxel
 288 sizes of 2.5 (c), 5 (d), 7.5 (e) and 10 (f) of plant communities with one (red) or four (blue) plant
 289 species ($N_{\text{one}} = 8$ plots, $N_{\text{four}} = 4$ plots). Bars show mean values (± 1 standard error); letters
 290 above bars indicate significant ($P < 0.05$) differences among treatments, letters in brackets
 291 indicate marginal significant ($0.05 < P < 0.1$) differences (Tukey's HSD test).



292

293 **Fig. 4** Fresh and dry biomass (a, b), and volume values obtained from voxel analysis with voxel
 294 sizes of 2.5 (c), 5 (d), 7.5 (e) and 10 (f) of plant communities without (green) or with (red)
 295 fertilization history (six plots, respectively). Bars show mean values (± 1 standard error); letters
 296 above bars indicate significant ($P < 0.05$) differences among treatments, letters in brackets
 297 indicate marginal significant ($0.05 < P < 0.1$) differences (Tukey's HSD test).

298 **Regressions between measured and determined variables**

299 We found highly significant positive linear relationships between biomass (fresh/dry) and
 300 volume (Table 2). The coefficient of determination R^2 was higher for fresh biomass ($R^2_{\text{mean}} =$
 301 0.85) than for dry biomass ($R^2_{\text{mean}} = 0.73$; Table 2). R^2 increased with larger voxel size, whereby
 302 this was more pronounced for dry biomass ($R^2 = 0.64-0.79$) than for fresh biomass ($R^2 = 0.82-$
 303 0.86; Table 2). We also found a significant positive relationship between measured and
 304 determined height (Table 2). If we removed one outlier (grass monoculture) from the analysis,
 305 R^2 was considerably higher (increase from $R^2 = 0.58$ to $R^2 = 0.81$; Table 2).

306

307 **Table 2** Results of mixed-effects model analyses testing for linear relationships between
 308 biomass (fresh or dry) and volume obtained from voxel analysis with voxel sizes of 2.5, 5, 7.5
 309 and 10 mm³, and between vegetation height measured in the field and height obtained from
 310 point cloud analysis. Shown are degrees of freedom (DF), Chi² values (χ^2), P values and
 311 coefficient of determination (R^2).

	DF	χ^2	P	R^2
Fresh biomass				
Biomass ~ Volume 2.5	1	19.80	<0.001	0.821
Biomass ~ Volume 5	1	21.81	<0.001	0.850
Biomass ~ Volume 7.5	1	22.01	<0.001	0.852
Biomass ~ Volume 10	1	22.64	<0.001	0.859
Dry biomass				
Biomass ~ Volume 2.5	1	11.65	<0.001	0.641
Biomass ~ Volume 5	1	15.41	<0.001	0.741
Biomass ~ Volume 7.5	1	16.68	<0.001	0.767
Biomass ~ Volume 10	1	17.64	<0.001	0.785
Vegetation height				
Measured height ~ determined height	1	9.89	0.002	0.583
Measured height ~ determined height (without B8A88)	1	17.31	<0.001	0.808

312

313 **Discussion**

314 Our study shows that traditional biomass harvesting and 3D scanning of vegetation with a
 315 smartphone produce similar results. Importantly, we found similar results of 3D-derived volume
 316 and dried biomass, which is commonly used as an estimate of plant productivity in ecological
 317 studies. High R^2 values between 0.7 and 0.9 show a good comparability between volume and
 318 dry biomass. The same applies to vegetation height. We conclude from our results that

319 smartphone 3D scanning can be a very useful approach to estimate biomass production and
320 vegetation height in a cheap, fast and almost non-destructive way. The method has several
321 advantages, in particular the simplicity of implementation, the widespread availability of
322 measurement devices (i.e. smartphones) as well as the free apps and analysis software.

323 From our experience, we can make the following recommendations regarding measurements in
324 the field and the subsequent processing of the point clouds:

- 325 • The frame is an important tool. Besides a well-defined area to scan, the frame also has the
326 advantage that nothing has to be cut off around the vegetation for proper scanning - so the
327 method is almost non-destructive. The frame should consist of wide boards so that the
328 vegetation growing around the focus area can be compressed (at least 25 cm wide).
- 329 • It is useful to scan the vegetation at least three times in a row because each scan produces
330 slightly different volumes (data not shown). To reduce this variability, multiple scans are
331 recommended.
- 332 • The processing of the point clouds is simple and can be realised with freely available
333 software. The corresponding script can be found under Elias, Dietrich and Bumberger
334 (2024). This workflow, in its current form, can be used immediately as a standard protocol
335 in research infrastructures, long-term experiments or in citizen science projects. The only
336 step that is not (yet) automated is the clipping of the point cloud to the region of interest.
- 337 • Our case study has shown that R^2 increases with voxel size, indicating that larger voxel sizes
338 lead to more realistic results. However, we found different effects of fertilisation history for
339 voxel size 10 mm^3 and fresh biomass. To increase certainty, we recommend using voxel
340 sizes larger than 2.5 mm^3 and smaller than 10 mm^3 , similar to previous findings (Enterkine
341 *et al.* 2023).

342 **Outlook**

343 Apart from biomass and height data, which can be reliably estimated with this technique, we
344 see great potential in developing this approach to derive further vegetation-related variables,
345 for example:

- 346 • segmentation of species in image data and semantic annotation including AI methods for
347 deriving species to determine the biomass production of individual species or functional
348 groups (e.g. grasses, herbs, legumes...) or to determine plant species richness
- 349 • detailed analysis of individual species or specific structures, such as leaves, through 'virtual
350 sampling,' which can yield insights into key ecological traits like leaf distribution and leaf
351 functional traits (e.g., specific leaf area)
- 352 • vertical distribution of different plant species or compartments (i.e. biomass allocation) in a
353 plant community
- 354 • assess the physiological state (e.g. drought response) of a plant community when dealing
355 with global change drivers, e.g. by deriving the proportion of living and dead plant material

356 This task will necessitate comprehensive research, including the modelling of the internal
357 structure of point clouds, potentially leveraging artificial intelligence and utilizing high-
358 resolution 3D scans of individuals from various species, encompassing different growth forms
359 and functional groups. Additionally, the data foundation must be expanded. One approach could
360 involve conducting measurements across multiple time points in various long-term
361 experiments, ideally within globally coordinated networks, to capture a diverse range of
362 vegetation types.

363 The direct next steps include further “ground-truthing” to estimate biomass from 3D point cloud
364 data, and to test reproducibility and comparisons to traditional methods, as well as scaling
365 opportunities to various more remotely-sensed imaging methods. Challenges are that the
366 resolution of the 3D scans is not very high and strongly depends on the quality of the used
367 smartphone (camera). Furthermore, the point clouds are quite noisy and require some, for now,

368 manual clipping and outlier removal. Thus, it is necessary to further develop the methods used
369 to automatically preprocess and analyse the point clouds. In addition, while it is currently
370 possible to detect effects of experimental treatments using volume data (e.g., differences in
371 species richness or fertilisation effect), further more comprehensive studies are needed to
372 determine exact biomass data (if an exact biomass estimate is required for a project), i.e. to
373 calibrate volume data (Enterkine *et al.* 2023).

374

375 **Conclusion**

376 Our pilot study demonstrates that scanning vegetation with a smartphone is a suitable
377 alternative to conventional biomass harvesting. At the same time, new insights can be gained,
378 for example by measuring biomass production over short time intervals or, in the future, non-
379 destructive measurement of vegetation structure or plant functional traits. Because of the
380 growing necessity for more and higher-quality vegetation data, we see that harnessing these
381 emerging technologies as an opportunity to meet the challenges of monitoring ecosystems,
382 opening up new questions and novel data to old questions, as well as a way to increase inclusion
383 and access to biodiversity science.

384

385 **Acknowledgement**

386 We thank the technicians at the Bad Lauchstädt field station for their support in maintaining the
387 experiment. We also appreciate the Helmholtz Centre for Environmental Research (UFZ) for
388 providing the smartphones and thank Anne Bienert for the helpful discussions on the Voxel
389 analysis.

390

391

392

393

394 **Data availability**

395 The original image data, the clipped image data, as well as the data processing scripts within a
396 Jupyter Notebook are published under an CC BY 4.0 license at Elias, Dietrich and Bumberger
397 (2024) and can be reused accordingly.

398

399 **References**

400 Barton, K. & Barton, M.K. (2015) Package ‘mumin’. *cran*, **1**, 1-79.

401 Bates, D., Mächler, M., Bolker, B. & Walker, S. (2014) Fitting linear mixed-effects models
402 using lme4. *arXiv* **1406.5823**. <https://doi.org/10.18637/jss.v067.i01>

403 Bienert, A., Georgi, L., Kunz, M., von Oheimb, G. & Maas, H.-G. (2021) Automatic
404 extraction and measurement of individual trees from mobile laser scanning point
405 clouds of forests. *Annals of Botany*, **128**, 787-804.
406 <https://doi.org/10.1093/aob/mcab087>

407 Bienert, A., Richter, K., Boehme, S. & Maas, H.-G. (2024) Investigating the Potential of
408 Hyper-Temporal Terrestrial Laser Point Clouds for Monitoring Deciduous Tree
409 Growth. *The International Archives of the Photogrammetry, Remote Sensing and*
410 *Spatial Information Sciences*, **48**, 33-40. [https://doi.org/10.5194/isprs-archives-](https://doi.org/10.5194/isprs-archives-XLVIII-2-2024-33-2024)
411 [XLVIII-2-2024-33-2024](https://doi.org/10.5194/isprs-archives-XLVIII-2-2024-33-2024)

412 Borer, E.T., Harpole, W.S., Adler, P.B., Lind, E.M., Orrock, J.L., Seabloom, E.W. & Smith,
413 M.D. (2014) Finding generality in Ecology: a model for globally distributed
414 experiments. *Methods in Ecology and Evolution*, **5**, 65-73.
415 <https://doi.org/10.1111/2041-210X.12125>

416 Cardinale, B.J., Duffy, J.E., Gonzalez, A., Hooper, D.U., Perrings, C., Venail, P., Narwani, A.,
417 Mace, G.M., Tilman, D., Wardle, D.A., Kinzig, A.P., Daily, G.C., Loreau, M., Grace,
418 J.B., Larigauderie, A., Srivastava, D.S. & Naeem, S. (2012) Biodiversity loss and its
419 impact on humanity. *Nature*, **486**, 59-67. <https://doi.org/10.1038/nature11148>

420 Chiappini, S., Balestra, M., Giulioni, F., Marcheggiani, E., Malinverni, E.S. & Pierdicca, R.
421 (2024) Comparing the accuracy of 3D urban olive tree models detected by smartphone
422 using LiDAR sensor, photogrammetry and NeRF: a case study of ‘Ascolana Tenera’ in
423 Italy. *ISPRS Annals of the Photogrammetry, Remote Sensing and Spatial Information*
424 *Sciences*, **10**, 61-68. <https://doi.org/10.5194/isprs-annals-X-3-2024-61-2024>

425 Cooper, S.D., Roy, D.P., Schaaf, C.B. & Paynter, I. (2017) Examination of the potential of
426 terrestrial laser scanning and structure-from-motion photogrammetry for rapid
427 nondestructive field measurement of grass biomass. *Remote Sensing*, **9**, 531.
428 <https://doi.org/10.3390/rs9060531>

429 Dandrifosse, S., Bouvry, A., Leemans, V., Dumont, B. & Mercatoris, B. (2020) Imaging wheat
430 canopy through stereo vision: Overcoming the challenges of the laboratory to field
431 transition for morphological features extraction. *Frontiers in plant science*, **11**, 96.
432 <https://doi.org/10.3389/fpls.2020.00096>

433 Demol, M., Verbeeck, H., Gielen, B., Armston, J., Burt, A., Disney, M., Duncanson, L.,
434 Hackenberg, J., Kükenbrink, D. & Lau, A. (2022) Estimating forest above-ground
435 biomass with terrestrial laser scanning: Current status and future directions. *Methods*
436 *in Ecology and Evolution*, **13**, 1628-1639. <https://doi.org/10.1111/2041-210X.13906>

437 Elias, M., Dietrich, P. & Bumberger, J. (2024) Advancing Plant Biomass Measurements:
438 Integrating Smartphone-based 3D Scanning Techniques for Enhanced Ecosystem
439 Monitoring [Data set]. *Zenodo*. <https://doi.org/10.5281/zenodo.14024991>

440 Enterkine, J., Hojatimalekshah, A., Vermillion, M., Van Der Weide, T., Arispe, S., Price, W.,
441 Hulet, A. & Glenn, N. (2023) Voxel Volumes and Biomass: estimating vegetation
442 volume and litter accumulation of exotic annual grasses using automated ultra-high
443 resolution SfM and advanced classification techniques. *Authorea Preprints*.
444 <https://doi.org/10.22541/au.169781950.03421718/v1>

445 Fischer, M., Bossdorf, O., Gockel, S., Hänsel, F., Hemp, A., Hessenmöller, D., Korte, G.,
446 Nieschulze, J., Pfeiffer, S. & Prati, D. (2010) Implementing large-scale and long-term
447 functional biodiversity research: The Biodiversity Exploratories. *Basic and Applied*
448 *Ecology*, **11**, 473-485. <https://doi.org/10.1016/j.baae.2010.07.009>

449 Habibullah, M.S., Din, B.H., Tan, S.-H. & Zahid, H. (2022) Impact of climate change on
450 biodiversity loss: global evidence. *Environmental Science and Pollution Research*, **29**,
451 1073-1086. <https://doi.org/10.1007/s11356-021-15702-8>

452 Hu, X., Li, Z., Miao, L., Fang, F., Jiang, Z. & Zhang, X. (2023) Measurement Technologies of
453 Light Field Camera: An Overview. *Sensors*, **23**, 6812.
454 <https://doi.org/10.3390/s23156812>

455 Keesing, F. & Ostfeld, R.S. (2021) Impacts of biodiversity and biodiversity loss on zoonotic
456 diseases. *Proceedings of the National Academy of Sciences*, **118**, e2023540118.
457 <https://doi.org/10.1073/pnas.2023540118>

458 Kobe, M., Elias, M., Merbach, I., Schädler, M., Bumberger, J., Pause, M. & Mollenhauer, H.
459 (2024) Automated Workflow for High-Resolution 4D Vegetation Monitoring Using
460 Stereo Vision. *Remote Sensing*, **16**, 541. <https://doi.org/10.3390/rs16030541>

461 Koedel, U., Schuetze, C., Fischer, P., Bussmann, I., Sauer, P.K., Nixdorf, E., Kalbacher, T.,
462 Wichert, V., Rechid, D. & Bouwer, L.M. (2022) Challenges in the evaluation of
463 observational data trustworthiness from a data producers viewpoint (FAIR+).
464 *Frontiers in Environmental Science*, **9**, 772666.
465 <https://doi.org/10.3389/fenvs.2021.772666>

466 Kolhar, S. & Jagtap, J. (2023) Plant trait estimation and classification studies in plant
467 phenotyping using machine vision—A review. *Information Processing in Agriculture*,
468 **10**, 114-135. <https://doi.org/10.1016/j.inpa.2021.02.006>

469 Kröhnert, M., Anderson, R., Bumberger, J., Dietrich, P., Harpole, W.S. & Maas, H.-G. (2018)
470 Watching grass grow—a pilot study on the suitability of photogrammetric techniques
471 for quantifying change in aboveground biomass in grassland experiments. *The*
472 *International Archives of the Photogrammetry, Remote Sensing and Spatial*
473 *Information Sciences*, **42**, 539-542. [https://doi.org/10.5194/isprs-archives-XLII-2-539-](https://doi.org/10.5194/isprs-archives-XLII-2-539-2018)
474 [2018](https://doi.org/10.5194/isprs-archives-XLII-2-539-2018)

475 Lausch, A., Heurich, M., Magdon, P., Rocchini, D., Schulz, K., Bumberger, J. & King, D.J.
476 (2020) A range of earth observation techniques for assessing plant diversity. *Remote*
477 *sensing of plant biodiversity*, 309-348. <https://doi.org/10.1007/978-3-030-33157-3>

478 López-Díaz, J., Roca-Fernández, A. & González-Rodríguez, A. (2011) Measuring herbage
479 mass by non-destructive methods: A review. *Journal of Agriculture, Science and*
480 *Technology*, **1**, 303-314.

481 Luetzenburg, G., Kroon, A. & Bjørk, A.A. (2021) Evaluation of the Apple iPhone 12 Pro
482 LiDAR for an application in Geosciences. *Scientific Reports*, **11**, 1-9.
483 <https://doi.org/10.1038/s41598-021-01763-9>

484 Micheletti, N., Chandler, J.H. & Lane, S.N. (2015) Investigating the geomorphological
485 potential of freely available and accessible structure-from-motion photogrammetry
486 using a smartphone. *Earth Surface Processes and Landforms*, **40**, 473-486.
487 <https://doi.org/10.1002/esp.3648>

488 Mollenhauer, H., Kasner, M., Haase, P., Peterseil, J., Wohner, C., Frenzel, M., Mirtl, M.,
489 Schima, R., Bumberger, J. & Zacharias, S. (2018) Long-term environmental
490 monitoring infrastructures in Europe: observations, measurements, scales, and socio-

491 ecological representativeness. *Science of the Total Environment*, **624**, 968-978.
492 <https://doi.org/10.1016/j.scitotenv.2017.12.095>

493 Ohnemus, T., Zacharias, S., Dirnböck, T., Bäck, J., Brack, W., Forsius, M., Mallast, U.,
494 Nikolaidis, N.P., Peterseil, J. & Piscart, C. (2024) The eLTER research infrastructure:
495 Current design and coverage of environmental and socio-ecological gradients.
496 *Environmental and Sustainability Indicators*, **23**, 100456.
497 <https://doi.org/10.1016/j.indic.2024.100456>

498 Richter, K. & Maas, H.-G. (2022) Radiometric enhancement of full-waveform airborne laser
499 scanner data for volumetric representation in environmental applications. *ISPRS*
500 *Journal of Photogrammetry and Remote Sensing*, **183**, 510-524.
501 <https://doi.org/10.1016/j.isprsjprs.2021.10.021>

502 Schima, R., Mollenhauer, H., Grenzdörffer, G., Merbach, I., Lausch, A., Dietrich, P. &
503 Bumberger, J. (2016) Imagine all the plants: Evaluation of a light-field camera for on-
504 site crop growth monitoring. *Remote Sensing*, **8**, 823.
505 <https://doi.org/10.3390/rs8100823>

506 Siebenkäs, A., Schumacher, J. & Roscher, C. (2016) Resource availability alters biodiversity
507 effects in experimental grass-forb mixtures. *PLoS One*, **11**, e0158110.
508 <https://doi.org/10.1371/journal.pone.0158110>

509 Smith, M.D., Wilkins, K.D., Holdrege, M.C., Wilfahrt, P., Collins, S.L., Knapp, A.K., Sala,
510 O.E., Dukes, J.S., Phillips, R.P. & Yahdjian, L. (2024) Extreme drought impacts have
511 been underestimated in grasslands and shrublands globally. *Proceedings of the*
512 *National Academy of Sciences*, **121**, e2309881120.
513 <https://doi.org/10.1073/pnas.2309881120>

514 Tilman, D., Knops, J., Wedin, D., Reich, P., Ritchie, M. & Siemann, E. (1997) The influence
515 of functional diversity and composition on ecosystem processes. *Science*, **277**, 1300-
516 1302. <https://doi.org/10.1126/science.277.5330.1300>

517 Tirrell, A.J., Putnam, A.E., Cianchette, M.I. & Gill, J.L. (2023) Using photogrammetry to
518 create virtual permanent plots in rare and threatened plant communities. *Applications*
519 *in Plant Sciences*, **11**, e11534. <https://doi.org/10.1002/aps3.11534>

520 Vinci, A., Todisco, F., Brigante, R., Mannocchi, F. & Radicioni, F. (2017) A smartphone
521 camera for the structure from motion reconstruction for measuring soil surface
522 variations and soil loss due to erosion. *Hydrology Research*, **48**, 673-685.
523 <https://doi.org/10.2166/nh.2017.075>

524 von Gönner, J., Herrmann, T.M., Bruckermann, T., Eichinger, M., Hecker, S., Klan, F., Lorke,
525 J., Richter, A., Sturm, U. & Voigt-Heucke, S. (2023) Citizen science's transformative
526 impact on science, citizen empowerment and socio-political processes. *Socio-*
527 *ecological practice research*, **5**, 11-33. <https://doi.org/10.1007/s42532-022-00136-4>

528 Weisser, W.W., Roscher, C., Meyer, S.T., Ebeling, A., Luo, G., Allan, E., Beßler, H., Barnard,
529 R.L., Buchmann, N. & Buscot, F. (2017) Biodiversity effects on ecosystem
530 functioning in a 15-year grassland experiment: Patterns, mechanisms, and open
531 questions. *Basic and Applied Ecology*, **23**, 1-73.
532 <https://doi.org/10.1016/j.baae.2017.06.002>

533 Zacharias, S., Loescher, H.W., Bogen, H., Kiese, R., Schrön, M., Attinger, S., Blume, T.,
534 Borchardt, D., Borg, E., Bumberger, J., Chwala, C., Dietrich, P., Fersch, B., Frenzel,
535 M., Gaillardet, J., Groh, J., Hajnsek, I., Itzerott, S., Kunkel, R., Kunstmann, H., Kunz,
536 M., Liebner, S., Mirtl, M., Montzka, C., Musolff, A., Pütz, T., Rebmann, C., Rinke, K.,
537 Rode, M., Sachs, T., Samaniego, L., Schmid, H.P., Vogel, H.-J., Weber, U.,
538 Wollschläger, U. & Vereecken, H. (2024) Fifteen Years of Integrated Terrestrial
539 Environmental Observatories (TERENO) in Germany: Functions, Services, and
540 Lessons Learned. *Earth's Future*, **12**, e2024EF004510.
541 <https://doi.org/10.1029/2024EF004510>

542